

---

# Delta-LLaVA: Base-then-Specialize Alignment for Token-Efficient Vision-Language Models

[Accepted at WACV 2026]

---

**Mohamad Zamini and Diksha Shukla, Senior Member, IEEE**

University of Wyoming

[mzamini@uwyo.edu](mailto:mzamini@uwyo.edu), [dshukla@uwyo.edu](mailto:dshukla@uwyo.edu)

## Abstract

Multimodal Large Language Models (MLLMs) combine visual and textual representations to enable rich reasoning capabilities. However, the high computational cost of processing dense visual tokens remains a major bottleneck. A critical component in this pipeline is the visual projector, which bridges the vision encoder and the language model. Standard designs often employ a simple multi-layer perceptron for direct token mapping, but this approach scales poorly with high-resolution inputs, introducing significant redundancy. We present Delta-LLaVA, a token-efficient projector that employs a low-rank DeltaProjection to align multi-level vision features into a compact subspace before further interaction. On top of this base alignment, lightweight Transformer blocks act as specialization layers, capturing both global and local structure under constrained token budgets. Extensive experiments and ablations demonstrate that this base-then-specialize design yields consistent gains across multiple benchmarks with only 144 tokens, highlighting the importance of token formation prior to scaling interaction capacity. With Delta-LLaVA, inference throughput improves by up to **55%**, while end-to-end training accelerates by nearly **4–5 $\times$**  in pretraining and over **1.5 $\times$**  in finetuning, highlighting the dual benefits of our design in both efficiency and scalability.

## 1 Introduction

Large language models have shown strong reasoning and generalization abilities. Recent multimodal models extends these capabilities to the visual domain. As universal interfaces, language models can follow natural language instructions while incorporating visual context. This enables general-purpose assistants that both perceive and reason about the world. Early multimodal systems such as Flamingo Alayrac et al. [2022], and more recent open-source efforts Li et al. [2024b], Team et al. [2024], Touvron et al. [2023], demonstrated that adding vision to pretrained language models greatly broadens the range of tasks they can solve. In most multimodal LLMs, images are converted into patch-based tokens by vision encoders like CLIP Radford et al. [2021]. These tokens are projected into the language space and then processed alongside text tokens Liu et al. [2023, 2024a]. While effective, this design often produces hundreds of tokens per image. As a result, visual processing becomes a major contributor to inference cost and latency.

A central bottleneck in this pipeline is the visual projector. Conventional projectors often adopt simple linear or MLP layers that retain all visual tokens, regardless of redundancy. This results in large token counts that overshadow textual prompts and inflate compute during both training and inference. Reducing the number of visual tokens has therefore become a primary research direction, with recent approaches proposing pooling layers, token merging, or lightweight attention mechanisms Chen et al. [2024b], Zhang et al. [2024], Li et al. [2024a]. However, these methods tend to compress features in ways that risk discarding fine-grained cues such as text regions, small objects, or structural



Figure 1: Grad-CAM visualization of the prompt: *What is weird about this picture?* The response (144 tokens) is: *The weird aspect of this picture is that a man is standing on the back of a yellow taxi while holding a clothes iron. This is unusual because it is not common to see someone using a clothes iron while standing on the back of a moving vehicle, especially a taxi. The man's actions seem unconventional and potentially dangerous, as he could lose his balance and fall off the taxi, causing injury or damage to the vehicle.* The images show results using 16, 64, and 144 visual tokens, from left to right (after the original image).

layout. The trade-off between reducing tokens and maintaining semantic fidelity remains a major challenge.

In this paper, we introduce Delta-LLaVA, a multimodal projector that addresses this challenge through a base-then-specialize design. At its core is a low-rank DeltaProjection layer that aligns multi-level vision features into a compact token subspace before any further processing. This base alignment establishes the representational foundation on which subsequent modules operate. On top of DeltaProjection, we integrate two specialization layers: an efficient multi-head self-attention (EMHSA) block that captures long-range dependencies under compressed token budgets, and a transformer block (TB) that injects local structure and inductive bias. In this design, DeltaProjection provides the critical alignment that determines the quality of the aggregate reasoning, while EMHSA and TB serve to refine and specialize the aligned tokens for task-specific demands.

Our analyses show that DeltaProjection causes the largest aggregate performance improvements across reasoning benchmarks, while removing EMHSA or TB produces smaller, task-dependent changes. For example, EMHSA contributes to long-range reasoning robustness, and TB yields modest gains in structured question answering, but both are secondary to the role of DeltaProjection. This pattern highlights the importance of investing model capacity in alignment layers that determine how tokens are formed, before allocating additional compute to interaction layers that determine how tokens are used. By enforcing this ordering, *Delta-LLaVA achieves competitive accuracy while substantially reducing FLOPS, advancing the efficiency of multimodal language models for real-world deployment.*

## 2 Related Work

Recent multimodal LLMs build on pretrained language models by coupling them with vision encoders such as CLIP Radford et al. [2021], EVA-CLIP Sun et al. [2023], or SigLIP-2 Tschannen et al. [2025]. These systems typically rely on a projector to map visual features into the language embedding space, enabling joint reasoning over text and images Liu et al. [2023], Alayrac et al. [2022], Li et al. [2023a]. While effective, this design often produces hundreds of tokens per image, inflating the sequence length seen by the LLM. Sequence compression has long been studied in purely textual models. Funnel Transformers Dai et al. [2020] reduce sequence length through pooling, while pruning methods Nawrot et al. [2022] dynamically remove redundant tokens. However, redundancy is more pronounced in images, where adjacent patches often encode overlapping or low-information content. This makes visual token compression especially attractive for multimodal models.

**Token pruning inside the LLM.** Some works reduce inference cost by pruning visual tokens after they enter the LLM. LLaVolta Chen et al. [2024a] adaptively pools and drops tokens across transformer layers, while EViT Liang et al. [2022] and Dynamic-ViT Rao et al. [2021] remove tokens within the vision backbone or multimodal stack. These methods save computation but require modifying or retraining the backbone, reducing modularity.

**Hierarchical and adaptive compression.** Some other studies propose adaptive or hierarchical compression. MQT Hu et al. [2024] and M3 Cai et al. [2024] employ Matryoshka representation learning Kusupati et al. [2022] to generate nested representations that adjust compute budgets at

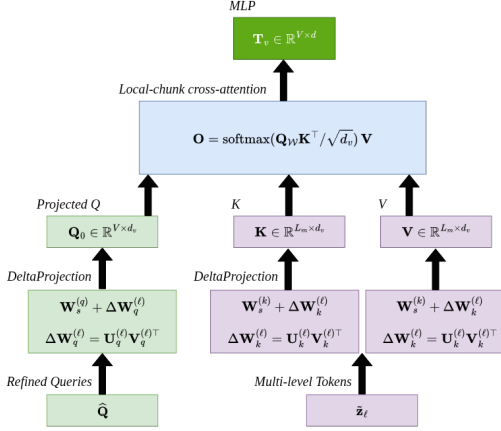


Figure 2: DeltaProjection inside Delta-LLaVA.

inference time. While flexible, these approaches may still propagate redundant tokens when operating at higher budgets.

**Projector-side compression.** A parallel direction which is our point of interest, compresses tokens before they reach the LLM. LLaVA-PruMerge Shang et al. [2024] selects salient patches using attention and merges redundant ones by clustering. Honeybee Cha et al. [2024] introduces a compact bottleneck, while TokenPacker Li et al. [2024c] uses coarse-to-fine attention to balance global and local detail. These methods are modular and LLM-agnostic, but still face a trade-off between efficiency and preservation of fine-grained semantics such as small text or layout.

Existing methods primarily frame compression as pruning or merging, with the risk of discarding task-critical information. In contrast, our work treats the projector as an alignment module rather than just a bottleneck. In our model, DeltaProjection as a base alignment layer, establishes a compact and semantically faithful token subspace. Ablations confirm that DeltaProjection is the principal driver of aggregate reasoning performance, while EMHSA and TB yield complementary, task-specific gains. This alignment-first, specialization-second perspective distinguishes our approach from prior projector-side compression methods.

### 3 Method

Multimodal LLMs aim to generate instruction-following responses from visual and textual inputs. They are generally composed of three key components:

- **Visual Encoder  $\mathcal{F}_I$ :** This module encodes an input image  $\mathbf{I}_{\text{img}} \in \mathbb{R}^{H \times W \times 3}$  into a sequence of visual embeddings  $\mathbf{I}_v \in \mathbb{R}^{N \times C}$ . Most current MLLMs employ CLIP-ViT-L/14 as the backbone, with patch size  $P = 14$ , resulting in  $N = HW/P^2$  visual tokens.
- **Visual Projector  $\Gamma_{I \rightarrow T}$ :** The visual projector serves as a crucial bridge between the vision and language models by translating visual features into visual tokens within a text embedding space that the language model can interpret. It transforms visual embeddings  $\mathbf{I}_v$  into a set of visual tokens  $\mathbf{T}_v$  within the language model’s embedding space  $\mathbb{T}$ , aligning the modalities for joint processing.
- **Language Model  $\Phi(\mathbf{T}_v, \mathbf{T}_t)$ :** The LLM receives both visual tokens  $\mathbf{T}_v$  and textual tokens  $\mathbf{T}_t$ , and generates responses autoregressively. Given a target sequence  $Y = \{y_i\}_{i=1}^L$ , the generation probability is defined as:

$$p(Y | \mathbf{T}_v, \mathbf{T}_t) = \prod_{i=1}^L p(y_i | \mathbf{T}_v, \mathbf{T}_t, y_{<i}) \quad (1)$$

While standard MLLM architectures are effective, their inference cost is jointly dictated by the number of visual tokens  $N$  and the size of the language model  $\Phi$ . Importantly, the computational

cost of  $\Phi(T_v, T_t)$  scales quadratically with the total number of tokens, making token count a critical factor in runtime efficiency. In this setting, the visual projector plays a central role: it transforms the  $N$  visual embeddings  $I_v$  into a set of  $M$  visual tokens  $T_v$ , which are passed to the language model.

Minimizing the number of visual tokens ( $M < N$ ) is therefore an essential strategy for improving inference efficiency. To this end, we introduce Delta-LLaVA, a visual projector that bridges the vision encoder and language model using as few tokens as possible.

## 4 Delta-LLaVA: Multimodal Projector

To reduce the number of visual tokens while preserving semantic fidelity, we introduce a Base-then-Specialize visual projection module that couples lightweight convolutional blocks with transformer-style attention. The Delta projector receives two streams from the vision tower: dense patch embeddings  $\mathbf{I}_v = \{\mathbf{z}_p\}_{p=1}^N$  and a compact multi-level summary  $\mathbf{I}_m = \{\tilde{\mathbf{z}}_\ell\}_{\ell=1}^{L_m}$ . Its task is to produce a *compressed* representation  $\mathbf{Y} \in \mathbb{R}^{V \times d}$ , with  $V \ll N$ , retaining the cues most predictive for the language model  $\Phi$ .

### 4.1 Query construction.

Let  $\mathbf{Z}$  denote patch-wise features on a raw  $\frac{H}{P} \times \frac{W}{P}$  grid. We first downsample this grid to  $\frac{H}{P_s} \times \frac{W}{P_s}$  via an interpolation operator  $Interp(\cdot)$ , where  $s \geq 1$  is the spatial scale. This preserves positional correspondences while reducing the query grid size. At the core of Delta-LLaVA is DeltaProjection, a low-rank projection inspired by a parameter-efficient adaptation method Mikaelyan et al. [2025].

Once alignment is established, Delta-LLaVA applies two specialization blocks for refining queries: 1) Multi-Head Convolutional Attention and 2) Efficient Multi-Head Self-Attention for capturing long-range dependencies with optional spatial reduction, enabling global context reasoning under compressed token budgets. Finally, we add fixed 2D sinusoidal positional embeddings.

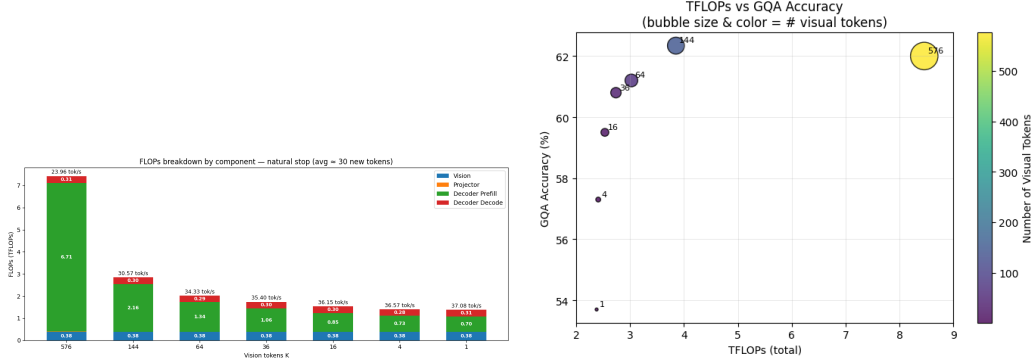
**Multi-Head Convolutional Attention (MHCA).** In our implementation, MHCA is a lightweight convolutional mixing block that approximates local attention while avoiding explicit dot–product computations. Instead of computing queries, keys, and values followed by a softmax, the input is processed by grouped  $3 \times 3$  depthwise convolutions (with the number of groups matching the number of heads), so that each head captures local spatial context in its own channel subset. The result is normalized with LayerNorm, passed through a ReLU activation, and then merged across heads with a convolution. A residual connection adds the input back to the output.

This design preserves the multi-head flavor of attention—each head aggregates a different local receptive field—while keeping the complexity linear in  $HW$ . MHCA therefore provides efficient locality modeling aligned with CNN inductive biases, without the quadratic overhead of token–token attention.

**Efficient Multi-Head Self-Attention (EMHSA).** To capture global semantics, we adopt a stabilized multi-head self-attention with pre-normalization and optional spatial reduction. Given normalized input  $\mathbf{X} \in \mathbb{R}^{B \times N \times C}$ , we form  $\mathbf{Q}, \mathbf{K}, \mathbf{V} \in \mathbb{R}^{B \times N \times C}$  and split them into  $H$  heads of dimension  $d = C/H$ . The attention is computed as

$$\text{Attn}(\mathbf{Q}, \mathbf{K}, \mathbf{V}) = \text{softmax}\left(\frac{\mathbf{Q}\mathbf{K}^\top}{\sqrt{d}}\right)\mathbf{V}. \quad (2)$$

For efficiency, when  $s > 1$  we downsample  $\mathbf{K}, \mathbf{V}$  to  $\mathbf{K}', \mathbf{V}' \in \mathbb{R}^{B \times (N/s^2) \times C}$ , reducing complexity from  $O(HN^2)$  to  $O(HN \cdot N/s^2)$  while preserving global receptive fields.



(a) Inference efficiency of the models on 100 samples. (b) Delta-LLaVA 144 tokens surpasses LLaVA-1.5 on Projector FLOPs are  $\leq 0.02$ .

Figure 3: Inference performance and accuracy with naturally terminated generations ( $\approx 30$  new tokens on average) under varying visual-token counts.

## 4.2 DeltaProjection.

The refined queries  $\hat{\mathbf{Q}}$  are then mapped into the vision–language embedding space with a DeltaLLM-style low-rank projection:

$$\hat{\mathbf{Q}} = \text{Refine}\left(\text{Interp}(\mathbf{Z}, \frac{H}{P_s}, \frac{W}{P_s})\right) + \text{Pos2D}, \quad (3)$$

$$\mathbf{Q}_0 = (\mathbf{W}_s + \Delta \mathbf{W}_q^{(\ell)}) \hat{\mathbf{Q}}, \quad \Delta \mathbf{W}_q^{(\ell)} = \mathbf{U}_q^{(\ell)} \mathbf{V}_q^{(\ell)\top}. \quad (4)$$

Here,  $\mathbf{W}_s \in \mathbb{R}^{d_v \times C}$  is a shared base weight, and  $\Delta \mathbf{W}_q^{(\ell)}$  is a lightweight, rank- $r$  update specific to layer  $\ell$ . The number of queries is

$$V = \frac{HW}{P_s^2 s^2}. \quad (5)$$

## 4.3 Coarse-to-fine mixing.

The projected queries  $\mathbf{Q}_0$  are then enriched by a cascade of transformer blocks (EMHSA  $\rightarrow$  MHCA  $\rightarrow$  MLP), followed by low-rank projection and local chunk attention:

$$\mathbf{Q} = \text{NTB}(\mathbf{Q}_0). \quad (6)$$

This cascade preserves resolution  $V$  while infusing each token with both local detail and long-range semantics.

This cascade preserves resolution  $V$  but enriches each token with information from both its immediate neighborhood and the full patch grid, enabling reasoning about fine details (object attributes, small text) while still capturing scene-level context.

**Key–value pathway.** In parallel to query construction, a compact set of multi-level feature tokens  $\tilde{\mathbf{z}}_\ell$  is transformed into keys and values via the same low-rank  $\Delta$ -projection used for queries. Let  $M = L_m$  denote the number of memory tokens. We obtain

$$\mathbf{K} = [\mathbf{k}_\ell]_{\ell=1}^M, \quad \mathbf{V} = [\mathbf{v}_\ell]_{\ell=1}^M, \quad (7)$$

$$\mathbf{k}_\ell = \text{Proj}_k(\tilde{\mathbf{z}}_\ell), \quad \mathbf{v}_\ell = \text{Proj}_v(\tilde{\mathbf{z}}_\ell), \quad (8)$$

where each  $\text{Proj}_\cdot$  is a shared base matrix plus a rank- $r$  Delta-LLaVA update (DeltaLLM-style Mikaelyan et al. [2025]), yielding parameter- and compute-efficient adaptation.

**Windowed cross-attention.** inspired by TokenPacker Li et al. [2024c], let the refined query sequence have length  $V = g^2$  (with  $g$  the query grid size after interpolation). We partition the query grid into non-overlapping windows  $\{\mathcal{W}_i\}$  of size  $w \times w$ , so there are  $V/w^2$  windows. Consistent

with the implementation, keys and values are downsampled/partitioned by the same spatial scale  $s$  to yield window-aligned subsets  $\mathbf{K}_{\mathcal{W}_i}, \mathbf{V}_{\mathcal{W}_i}$ . Within each window we compute

$$\mathbf{O}_{\mathcal{W}_i} = \text{softmax}\left(\frac{\mathbf{Q}_{\mathcal{W}_i} \mathbf{K}_{\mathcal{W}_i}^\top}{\sqrt{d}}\right) \mathbf{V}_{\mathcal{W}_i}, \quad (9)$$

$$\mathbf{Y} = [\mathbf{O}_{\mathcal{W}_i}]_{i=1}^{V/w^2}, \quad (10)$$

where  $d$  is the per-head dimension. This *local chunk attention* reduces quadratic cost by restricting interactions to spatial neighborhoods while anchoring every window to the compact multi-level memory.

Table 1: Comparison of token compression methods across varying compression rates. All models use the Vicuna-1.5 7B backbone unless otherwise specified. The best and second-best results are highlighted in bold and underline, respectively. Our method achieves superior performance under extreme compression and remains competitive at moderate levels. Results for 1–36 tokens are taken from Li et al. [2024a]; the rest are reported from the original papers. A dash (–) indicates that results were not reported for the corresponding benchmark.

Method	# Token	GQA	MMB	MME	POPE	SQA	TextVQA	VizWiz	VQAv2
LLaVA-1.5	576	<b>62.0</b>	64.3	<b>1510.7</b>	85.9	66.8	<b>58.2</b>	50.0	<b>78.5</b>
TokenPacker	144	61.9	<u>65.1</u>	–	<b>87.0</b>	–	–	52.0	<u>77.9</u>
Matryoshka Multi.	144	61.3	<b>66.4</b>	–	<b>87.0</b>	–	–	<u>53.1</u>	–
Matryoshka Query	144	61.4	64.4	1446.5	83.9	<u>67.5</u>	–	52.0	76.4
<b>Delta-LLaVA (Ours)</b>	144	<b>62.34</b>	<u>65.95</u>	<u>1466.52</u>	<u>86.77</u>	<b>68.7</b>	57.14	<b>56.6</b>	76.1
<b>LLaVA-1.5 13B</b>	576	<b>63.3</b>	<b>67.7</b>	<b>1531.3</b>	86.2	<b>71.6</b>	<b>61.3</b>	53.6	<b>80.0</b>
<b>Delta-LLaVA-13B (Ours)</b>	144	62.7	67.4	1527.41	<b>87.3</b>	<b>71.6</b>	59.25	<b>58.2</b>	76.9
PruMerge	~32	57.2	60.9	1350.3	76.3	68.5	<b>56.0</b>	45.2	72.0
TokenPacker	36	59.6	62.8	<u>1440.9</u>	83.3	<b>71.0</b>	53.2	50.2	<u>75.0</u>
Matryoshka Multi.	36	60.3	<b>64.8</b>	–	<u>85.5</u>	–	–	<u>52.8</u>	–
Matryoshka Query	36	58.8	63.4	1416.3	81.9	66.8	–	51.0	73.7
QueCC	36	<u>60.5</u>	62.5	<b>1442.0</b>	84.5	<u>70.6</u>	53.3	50.1	<b>75.8</b>
<b>Delta-LLaVA (Ours)</b>	36	<b>61</b>	<u>64.4</u>	1424.7	<b>85.7</b>	68.6	<u>54.4</u>	<b>56.2</b>	74.3
TokenPacker	16	58.9	<u>62.7</u>	1378.8	<u>83.7</u>	68.1	<u>52.5</u>	50.5	<u>74.4</u>
Matryoshka Query	16	57.6	<u>61.9</u>	<b>1408.5</b>	80.8	67.5	–	49.8	<u>71.1</u>
QueCC	16	<u>59.0</u>	62.2	<u>1408.0</u>	83.4	<b>70.7</b>	51.3	47.7	<b>74.5</b>
<b>Delta-LLaVA (Ours)</b>	16	<b>59.5</b>	<b>62.9</b>	1375.9	<b>84.7</b>	<u>69.7</u>	<b>53.6</b>	<b>55.2</b>	73.1
TokenPacker	4	56.2	61.5	<u>1347.6</u>	81.7	<u>68.5</u>	<u>49.2</u>	45.7	70.5
Matryoshka Query	4	53.0	56.5	1176.1	77.6	<u>65.1</u>	–	<u>49.4</u>	64.1
QueCC	4	<u>56.5</u>	<b>62.1</b>	<b>1390.3</b>	<u>81.8</u>	<b>68.6</b>	48.7	<u>45.0</u>	<u>70.6</u>
<b>Delta-LLaVA (Ours)</b>	4	<b>57.3</b>	<u>61.7</u>	1314.2	<b>82.2</b>	67.9	<b>53.1</b>	<b>52.6</b>	<b>72.0</b>
TokenPacker	1	53.4	58.7	<b>1262.4</b>	80.7	<u>69.4</u>	46.2	41.1	<b>66.9</b>
Matryoshka Multi.	1	52.6	<b>59.5</b>	–	78.4	–	–	<u>49.4</u>	–
Matryoshka Query	2	50.8	54.4	1144.0	74.5	65.0	–	48.5	61.0
QueCC	1	<u>53.5</u>	<u>59.4</u>	<u>1269.1</u>	<u>81.3</u>	<b>69.9</b>	<u>46.8</u>	44.1	<u>67.3</u>
<b>Delta-LLaVA (Ours)</b>	1	<b>53.7</b>	57.6	1257.9	<b>82.4</b>	68.7	<b>48</b>	<b>51</b>	66.1

- **Low-rank projections.** Both  $\text{Proj}_k$  and  $\text{Proj}_v$  share the same  $\Delta$ -form as the query projection (shared base + rank- $r$  update).
- **Compact memory.** Since  $M \ll V$ , the key–value cache remains small relative to the query sequence, keeping the memory branch lightweight.
- **Efficiency.** Combining localized attention with a compact memory provides fine spatial reasoning and long-range context at much lower cost than global self-attention.

#### 4.4 Feed-forward refinement.

Finally, a position-wise two-layer MLP with hidden width  $h = 4096$  refines the tokens:

$$\mathbf{T}_v = \mathbf{T}_v + \mathbf{W}_2 \sigma(\mathbf{W}_1 \text{LN}(\mathbf{T}_v)). \quad (11)$$

This residual feed-forward path enhances non-linear expressivity while maintaining stability.

## 5 FLOPs Analysis.

Let  $V_0 = \frac{HW}{P^2}$  be the raw patch-token count and  $V = \frac{V_0}{s^2}$  the post-compression tokens at spatial scale  $s$ . We separate vision/projector from LLM prefill/decode.

**Projector.** The proposed Delta-LLaVA projector includes low-rank projections, convolutional blocks, windowed attention, and feed-forward refinement. For fixed embedding dimension  $d$ , rank  $r$ , and local window size  $L_m$ , the dominant terms are

- low-rank projections:  $\mathcal{O}(Vd)$ ,
- convolutional mixing (MHCA):  $\mathcal{O}(Vdk^2)$ ,
- feed-forward MLP:  $\mathcal{O}(Vrd^2)$ ,
- local/windowed attention:  $\mathcal{O}(VL_md)$ .

Each term scales *linearly* with  $V$ , so the overall projector complexity is

$$F_{\text{proj}}(s) = \Theta(V) = \Theta\left(\frac{V_0}{s^2}\right). \quad (12)$$

For fixed  $d$  (embed dim), expansion ratio  $r$ , kernel size  $k$ , and local window  $L_m$ , the dominant terms are

$$\mathcal{O}(Vd) + \mathcal{O}(Vdk^2) + \mathcal{O}(Vrd^2) + \mathcal{O}(VL_md) = \Theta(V). \quad (13)$$

Thus, doubling the scale factor  $s$  reduces projector FLOPs by a factor of four, in contrast to global self-attention which scales quadratically  $\Theta(V^2d)$ .

**LLM Prefill.** With  $T$  text tokens, the prefill context length is  $S_0 = T + V$ . Per layer,

$$F_{\text{prefill}}(T, V) = \Theta(S_0 rd^2) + \Theta(S_0^2 d). \quad (14)$$

In 7B-class models the MLP term  $\Theta(S_0 rd^2)$  dominates, so prefill FLOPs scale approximately linearly with  $V$ . This matches our measurements:  $F_{\text{prefill}}$  drops from 6.72 TFLOPs at  $V=576$  to 2.16 (@144), 0.85 (@16), and 0.70 (@1).

**LLM Decode.** With KV caching, generating  $G$  tokens yields per-layer cost

$$F_{\text{decode}}(T, V, G) = \Theta(G rd^2) + \Theta(G S_0 d). \quad (15)$$

Because the MLP term dominates,  $F_{\text{decode}}$  is nearly constant in  $V$ . In our natural-stop runs ( $G \approx 30$  on average), decode FLOPs range only from 0.31 TFLOPs (@576) to 0.28 (@4–16). Runtime per generated token shows modest variation: tokens/sec rises from  $\approx 24$  (@576) to  $\approx 37$  (@1), a  $\sim 55\%$  gain, even though decode FLOPs remain flat.

**Vision Encoder.**  $F_{\text{vision}}$  is effectively constant (e.g., 0.382 TFLOPs in all settings), since compression happens post-backbone.

The total complexity is

$$\begin{aligned} F_{\text{total}}(V) \approx & F_{\text{vision}} + F_{\text{proj}}(V) + F_{\text{prefill}}(T, V) \\ & + F_{\text{decode}}(T, V, G). \end{aligned} \quad (16)$$

Reducing  $V$  meaningfully cuts projector and *prefill* FLOPs (and KV memory), but *decode* FLOPs stay nearly constant and decode *runtime* is limited by KV-cache read bandwidth. For long generations ( $G \gg T + V$ ), decode dominates inference time, so reducing  $V$  has negligible impact on end-to-end latency.

## 6 Experiments

**Model Setup.** We adopt LLaVA-1.5 as the foundation for our multimodal language models (MLLMs), integrating various language backbones including Vicuna-7B, Vicuna-13B, Qwen-7B. For vision encoding, we employ CLIP-ViT-B/32 (224) and CLIP-ViT-L/14 (336). All models are trained for one epoch using  $8 \times$  NVIDIA H100 GPUs.

**Evaluation Benchmarks.** We follow a two-stage training pipeline. The Delta-LLaVA module is first trained on CC-558K Liu et al. [2023] for modality alignment. We then apply instruction tuning using the 665K LLaVA mixture Liu et al. [2024a]. Evaluation is performed on a diverse suite of benchmarks using LMMs-Eval tool Zhang et al. [2025]: general VQA tasks ( $VQA^v2$  Goyal et al. [2017], GQA Hudson and Manning [2019], VizWiz Gurari et al. [2018]); hallucination detection (POPE Li et al. [2023b]); comprehensive reasoning benchmarks (MMBench Liu et al. [2024b], MME Liang et al. [2024]); and image captioning (Nocaps Agrawal et al. [2019] and Flickr30KPlummer et al. [2015]).

### 6.1 Empirical Analysis.

Table 1 compares token compression strategies across a wide range of visual token counts. At the full setting of 576 tokens, the baseline LLaVA-1.5 achieves strong performance, particularly on MME (1510.7) and VQAv2 (78.5). However, as tokens are reduced, most baselines experience steep accuracy drops, especially below 16 tokens. Our method, Delta-LLaVA, consistently outperforms or closely matches competing approaches across all compression levels. At moderate compression (144 tokens), Delta-LLaVA improves GQA (62.34 vs. 61.9 TokenPacker) and SQA (68.7 vs. 67.5 Matryoshka Query), while preserving competitive scores on MME and POPE. At aggressive compression (36 and 16 tokens), Delta-LLaVA delivers the best or second-best results in the majority of benchmarks, notably maintaining VizWiz performance (56.2 at 36 tokens, 55.2 at 16 tokens) where others degrade. Even at extreme settings of 4 or 1 token, Delta-LLaVA remains robust, achieving the top scores on GQA, POPE, TextVQA, and VizWiz, highlighting its resilience under severe token bottlenecks. Notably, scaling Delta-LLaVA to a 13B backbone further boosts overall accuracy, suggesting complementary gains from larger language capacity. These results demonstrate that Delta-LLaVA achieves state-of-the-art trade-offs between efficiency and performance, particularly excelling at extreme compression where prior methods collapse.

Method	# Token	GQA	MMB	MME	POPE	SQA	VizWiz
Qwen-VL-Chat	448	57.5	60.6	1487.5	68.2	38.9	<b>78.2</b>
<b>Delta-LLaVA Qwen</b>	144	<b>61.77</b>	<b>72.0</b>	<b>1524.0</b>	<b>87.0</b>	<b>73.1</b>	<b>41.7</b>
<b>Delta-LLaVA Qwen</b>	36	55.1	<u>67.3</u>	1452.3	86.2	<u>72.4</u>	33.1

Table 2: Results obtained using the LLaVA architecture with Qwen-7B as the language model compared to Qwen-VL-Chat.

Table 2 compares Delta-LLaVA with Qwen-7B as the language model against the baseline Qwen-VL-Chat. Despite using significantly fewer visual tokens (144 vs. 448), Delta-LLaVA Qwen delivers clear improvements across most benchmarks, achieving the best scores on GQA, MMB, MME, POPE, SQA, and VizWiz. Notably, the 144-token variant surpasses the baseline by more than 3 points on GQA and over 11 points on MMB, while also increasing MME to 1524.0. Even under extreme compression to 36 tokens, Delta-LLaVA Qwen maintains competitive performance, with only modest drops in accuracy relative to the full-token baseline. These results demonstrate that the Delta-LLaVA framework can drastically reduce the visual token budget while enhancing reasoning performance, highlighting both efficiency and robustness compared to Qwen-VL-Chat.

### 6.2 Ablation Study

To evaluate the contribution of each component in our proposed architecture, we conducted an ablation study by selectively removing individual modules. Table 3 reports performance across five benchmarks: GQA, MMB (Reasoning), MME (Reasoning), POPE (Hallucination), and SQA.

The results highlight that each module contributes differently. Removing E-MHSA reduces reasoning performance (MMB, MME) but yields the highest POPE score, suggesting that global self-attention

Model	GQA	MMB	MME	POPE	SQA
No EMHSA	61.07	<b>64.77</b>	<u>1449.84</u>	<b>88.0</b>	68.17
No DeltaProj	61.47	62.71	1431.67	85.57	68.32
No TB	62.0	64.17	1422.42	<u>86.83</u>	<b>70.20</b>
Full Model	<b>62.34</b>	<b>65.95</b>	<b>1466.52</b>	86.77	68.67

Table 3: Ablation study across reasoning and hallucination benchmarks. We removed one module and kept the rest each time. Bold values indicate the best performance within each column.

aids reasoning but may also amplify hallucinations. Eliminating DeltaProjection consistently lowers reasoning metrics, demonstrating the importance of low-rank query alignment for efficient cross-modal fusion. Removing TB slightly decreases MME performance but surprisingly improves SQA, indicating that some linguistic tasks benefit from a simplified local representation. Overall, the full model achieves the best balance across tasks, with strong reasoning ability (MMB, MME) and competitive hallucination control (POPE).

### 6.3 Training Efficiency

We report end-to-end wall-clock time for both pretraining and instruction finetuning across different Delta-LLaVA variants in Table 4. All experiments were conducted under identical hardware and dataloader configurations to isolate the effect of token compression on efficiency.

Model	Pretraining	Finetuning
LLaVA 576	1:24:01	4:34:20
LLaVA 144	0:33:32	3:21:37
LLaVA 64	0:23:24	3:17:23
LLaVA 16	0:18:36	3:14:29
LLaVA 4	0:16:32	3:12:34
LLaVA 1	0:16:00	2:51:50

Table 4: Training speed comparison across variants. Reported as wall-clock time for one epoch of pretraining and finetuning.

We observe a clear monotonic reduction in training time as the number of visual tokens decreases. Standard LLaVA requires more than 3.5 hours for pretraining and over 7.5 hours for finetuning per epoch, whereas our most compressed variant (LLaVA 1) reduces these to 16 minutes and 2.9 hours, respectively. This corresponds to a  $\sim 13\times$  speedup in pretraining and more than  $2.5\times$  acceleration in finetuning.

Interestingly, the majority of gains are realized during the pretraining stage, where visual encoding dominates compute. As token count is reduced (e.g., from 144 down to 1), the quadratic attention cost shrinks substantially, leading to near-linear savings in wall-clock time. In contrast, finetuning benefits less dramatically since language-heavy updates dominate compute at this stage.

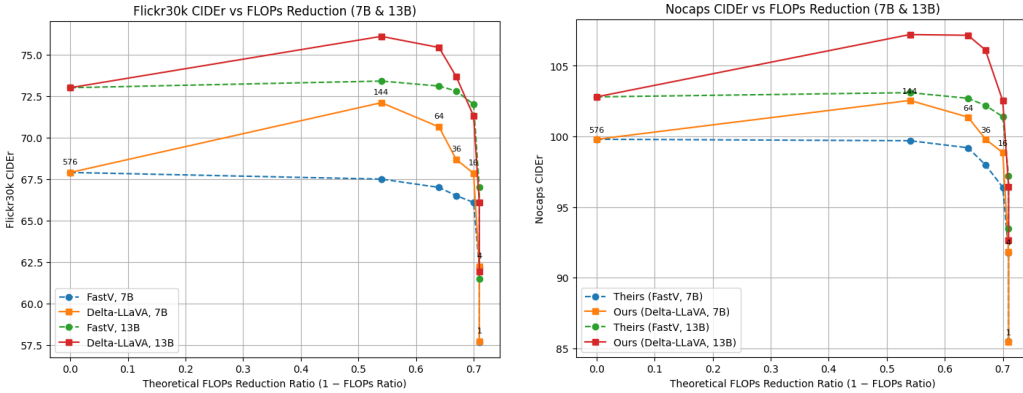
Overall, these results demonstrate that Delta-LLaVA yields significant efficiency improvements without sacrificing downstream performance, making it particularly attractive for scaling multimodal training under limited GPU budgets.

### 6.4 Delta-LLaVA with different Vision Towers Analysis

Table 5 compares the performance of different vision towers when paired with the Vicuna-7B backbone under a fixed token budget. Both CLIP-based models achieve strong results, with CLIP-336 slightly outperforming CLIP-224 on most benchmarks, particularly on GQA and POPE, while CLIP-224 shows a modest advantage on SQA. SigLIP-386, despite processing more tokens (81 vs. 64), trails behind on most tasks, especially on MME and MMB, though it remains competitive on POPE and SQA. These results highlight that increasing the resolution or token count does not guarantee better performance, and that CLIP-based towers provide a more balanced trade-off between accuracy across datasets and computational efficiency.

Vision Tower	# Token	GQA	MMB	MME	POPE	SQA	VizWiz
<b>CLIP 336</b>	64	<b>61.1</b>	<b>64.94</b>	1442	<b>86.12</b>	67.82	<b>57.2</b>
<b>CLIP 224</b>	64	60.5	64.9	<b>1448.1</b>	84.56	69.3	56.1
<b>SigLIP 386</b>	81	59.44	61.69	1345.03	85.2	<b>68.42</b>	55.54

Table 5: Results obtained using the Vicuna 7B and with different vision towers.



(a) Flickr30k CIDEr under pruning. Delta-LLaVA (solid) consistently achieves higher scores than FastV preserves captioning quality significantly better than (dashed) across both 7B and 13B.

(b) Nocaps CIDEr under pruning. Delta-LLaVA (solid) preserves captioning quality significantly better than FastV at both 7B and 13B.

Figure 4: Comparison of captioning robustness under token pruning. Across Flickr30k and Nocaps benchmarks, Delta-LLaVA achieves a superior accuracy–efficiency trade-off relative to FastV, especially at moderate to aggressive pruning levels.

## 6.5 Visual Token Pruning on Inference Efficiency

We evaluate how pruning the number of vision tokens  $K$  passed from the vision tower to the LLM affects inference when generation is allowed to stop naturally (averaging  $\sim 30$  new tokens). We sweep  $K \in \{576, 144, 64, 36, 16, 4, 1\}$ . Figure 3 reports both total compute (stacked by component) and tokens-per-second (TPS), with TPS values annotated above each bar.

**Observed behavior.** TPS improves as  $K$  decreases—from 23.96 tok/s at  $K=576$  to  $\approx 36$ –37 tok/s for  $K \leq 16$  (peak 37.08 tok/s at  $K=1$ ;  $\sim 55\%$  gain). In contrast, total FLOPs drop sharply: 7.43 TFLOPs at  $K=576$ , 2.84 at 144, and 1.74–1.39 for  $K \leq 36$  ( $\sim 81\%$  reduction from 576  $\rightarrow$  1). The breakdown shows that pruning mainly reduces decoder *prefill* cost (scales with  $T+K$ ), falling from 6.72 TFLOPs ( $K=576$ ) to 0.70 TFLOPs ( $K=1$ ). The *decode* stage remains nearly constant across  $K$  ( $\approx 0.28$ –0.31 TFLOPs for  $\sim 30$  generated tokens). The vision encoder is fixed by input resolution ( $\approx 0.382$  TFLOPs), and the projector is negligible ( $\leq 0.002$  TFLOPs except 0.024 at  $K=576$ ).

## 6.6 Performance of Delta-LLaVA in image captioning tasks

Our results in Table 6 demonstrate that Delta-LLaVA outperforms FastV Chen et al. [2024b] across both Nocaps and Flickr30k CIDEr benchmarks for LLaVA-1.5-7B and 13B. At baseline (576 tokens), performance is matched, but once pruning is applied our models maintain higher scores at all levels—with particularly large margins at moderate pruning (e.g., 144–64 tokens), where Delta-LLaVA achieves up to 3–5 CIDEr points higher. This indicates that our approach is especially well-suited for captioning-style tasks (Nocaps, Flickr30k), where preserving fine-grained visual grounding under compression is critical. Even under extreme pruning ( $K=1$ –4), our curves degrade more gracefully, retaining  $\geq 85\%$  of baseline performance, while FastV shows sharper declines. Together, these findings highlight Delta-LLaVA as a more robust token-efficient model, delivering stronger accuracy–efficiency trade-offs for vision–language tasks where captioning fidelity and robustness to compression are essential, without sacrificing inference efficiency.

# Tokens	LLaVA-1.5-7B				LLaVA-1.5-13B			
	Nocaps		CIDEr		Nocaps		CIDEr	
	FastV	Ours	FastV	Ours	FastV	Ours	FastV	Ours
576	99.8	99.8	67.9	67.9	102.8	102.8	73.0	73.0
144	99.7	<b>102.6</b>	67.5	<b>72.1</b>	103.1	<b>107.2</b>	73.4	<b>76.1</b>
64	99.2	<b>101.4</b>	67.0	<b>70.6</b>	102.7	<b>107.2</b>	73.1	<b>75.4</b>
36	98.0	<b>99.8</b>	66.5	<b>68.7</b>	102.2	<b>106.1</b>	72.8	<b>73.7</b>
16	96.4	<b>98.9</b>	66.1	<b>67.9</b>	101.4	<b>102.5</b>	<b>72.0</b>	71.3
4	91.8	<b>91.9</b>	62.2	<b>62.2</b>	<b>97.2</b>	96.5	<b>67.0</b>	66.1
1	85.5	<b>85.5</b>	57.7	<b>57.7</b>	<b>93.5</b>	92.7	61.5	<b>61.9</b>

Table 6: Comparison of Nocaps and Flickr30k CIDEr scores under pruning for LLaVA-1.5-7B and LLaVA-1.5-13B. We report results from FastV and our Delta-LLaVA implementation (“Ours”). Token counts  $K$  correspond to the number of visual tokens retained.

## 7 Conclusion

Our experiments demonstrate that Delta-LLaVA sets a new standard for token-efficient multimodal modeling. By introducing the Delta Projector, which combines low-rank alignment with lightweight specialization layers, the model achieves stronger reasoning performance and robustness under severe visual token compression.

Across benchmarks, Delta-LLaVA sustains competitive or superior accuracy even when the number of visual tokens is reduced by orders of magnitude. At moderate compression (e.g., 144 tokens), it surpasses strong baselines on tasks such as GQA, Nocaps, and Flickr30K, while at aggressive settings (36–16 tokens) it attains the best or second-best scores on GQA, VizWiz, SQA, and POPE. Remarkably, the model remains resilient at extreme compression (4–1 tokens), where prior methods fail. Scaling to larger LLM backbones further amplifies these gains, underscoring the synergy between stronger language capacity and efficient visual projection.

Efficiency analyses confirm that compressing vision tokens not only reduces FLOPs by up to 70% ( $576 \rightarrow 1$  token), but also accelerates training by more than  $4 - 5 \times$  during pretraining and over  $1.5 \times$  during instruction tuning. These results highlight the importance of principled token formation for building scalable and efficient multimodal large language models.

## References

Harsh Agrawal, Karan Desai, Yufei Wang, Xinlei Chen, Rishabh Jain, Mark Johnson, Dhruv Batra, Devi Parikh, Stefan Lee, and Peter Anderson. Nocaps: Novel object captioning at scale. In *Proceedings of the IEEE/CVF international conference on computer vision*, pages 8948–8957, 2019.

Jean-Baptiste Alayrac, Jeff Donahue, Pauline Luc, Antoine Miech, Iain Barr, Yana Hasson, Karel Lenc, Arthur Mensch, Katherine Millican, Malcolm Reynolds, et al. Flamingo: a visual language model for few-shot learning. *Advances in neural information processing systems*, 35:23716–23736, 2022.

Mu Cai, Jianwei Yang, Jianfeng Gao, and Yong Jae Lee. Matryoshka multimodal models. In *Workshop on Video-Language Models@ NeurIPS 2024*, 2024.

Junbum Cha, Wooyoung Kang, Jonghwan Mun, and Byungseok Roh. Honeybee: Locality-enhanced projector for multimodal ilm. In *Proceedings of the IEEE/CVF Conference on Computer Vision and Pattern Recognition*, pages 13817–13827, 2024.

Jieneng Chen, Luoxin Ye, Ju He, Zhao-Yang Wang, Daniel Khashabi, and Alan Yuille. Lla-volta: Efficient multi-modal models via stage-wise visual context compression. *arXiv preprint arXiv:2406.20092*, 2024a.

Liang Chen, Haozhe Zhao, Tianyu Liu, Shuai Bai, Junyang Lin, Chang Zhou, and Baobao Chang. An image is worth 1/2 tokens after layer 2: Plug-and-play inference acceleration for large vision-language models. In *European Conference on Computer Vision*, pages 19–35. Springer, 2024b.

Zihang Dai, Guokun Lai, Yiming Yang, and Quoc Le. Funnel-transformer: Filtering out sequential redundancy for efficient language processing. *Advances in neural information processing systems*, 33:4271–4282, 2020.

Yash Goyal, Tejas Khot, Douglas Summers-Stay, Dhruv Batra, and Devi Parikh. Making the v in vqa matter: Elevating the role of image understanding in visual question answering. In *Proceedings of the IEEE conference on computer vision and pattern recognition*, pages 6904–6913, 2017.

Danna Gurari, Qing Li, Abigale J Stangl, Anhong Guo, Chi Lin, Kristen Grauman, Jiebo Luo, and Jeffrey P Bigham. Vizwiz grand challenge: Answering visual questions from blind people. In *Proceedings of the IEEE conference on computer vision and pattern recognition*, pages 3608–3617, 2018.

Wenbo Hu, Zi-Yi Dou, Liunian Harold Li, Amita Kamath, Nanyun Peng, and Kai-Wei Chang. Matryoshka query transformer for large vision-language models. *arXiv preprint arXiv:2405.19315*, 2024.

Drew A Hudson and Christopher D Manning. Gqa: A new dataset for real-world visual reasoning and compositional question answering. In *Proceedings of the IEEE/CVF conference on computer vision and pattern recognition*, pages 6700–6709, 2019.

Aditya Kusupati, Gantavya Bhatt, Aniket Rege, Matthew Wallingford, Aditya Sinha, Vivek Rammanujan, William Howard-Snyder, Kaifeng Chen, Sham Kakade, Prateek Jain, et al. Matryoshka representation learning. *Advances in Neural Information Processing Systems*, 35:30233–30249, 2022.

Junnan Li, Dongxu Li, Silvio Savarese, and Steven Hoi. Blip-2: Bootstrapping language-image pre-training with frozen image encoders and large language models. In *International conference on machine learning*, pages 19730–19742. PMLR, 2023a.

Kevin Y Li, Sachin Goyal, Joao D Semedo, and J Zico Kolter. Inference optimal vlms need only one visual token but larger models. *arXiv preprint arXiv:2411.03312*, 2024a.

Teng Li, Jiapeng Wang, and Lianwen Jin. Enhancing visual information extraction with large language models through layout-aware instruction tuning. In *Chinese Conference on Pattern Recognition and Computer Vision (PRCV)*, pages 276–289. Springer, 2024b.

Wentong Li, Yuqian Yuan, Jian Liu, Dongqi Tang, Song Wang, Jie Qin, Jianke Zhu, and Lei Zhang. Tokenpacker: Efficient visual projector for multimodal llm. *arXiv preprint arXiv:2407.02392*, 2024c.

Yifan Li, Yifan Du, Kun Zhou, Jinpeng Wang, Wayne Xin Zhao, and Ji-Rong Wen. Evaluating object hallucination in large vision-language models. *arXiv preprint arXiv:2305.10355*, 2023b.

Youwei Liang, Chongjian Ge, Zhan Tong, Yibing Song, Jue Wang, and Pengtao Xie. Not all patches are what you need: Expediting vision transformers via token reorganizations. *arXiv preprint arXiv:2202.07800*, 2022.

Zijing Liang, Yanjie Xu, Yifan Hong, Penghui Shang, Qi Wang, Qiang Fu, and Ke Liu. A survey of multimodel large language models. In *Proceedings of the 3rd International Conference on Computer, Artificial Intelligence and Control Engineering*, pages 405–409, 2024.

Haotian Liu, Chunyuan Li, Qingyang Wu, and Yong Jae Lee. Visual instruction tuning. *Advances in neural information processing systems*, 36:34892–34916, 2023.

Haotian Liu, Chunyuan Li, Yuheng Li, and Yong Jae Lee. Improved baselines with visual instruction tuning. In *Proceedings of the IEEE/CVF Conference on Computer Vision and Pattern Recognition*, pages 26296–26306, 2024a.

Yuan Liu, Haodong Duan, Yuanhan Zhang, Bo Li, Songyang Zhang, Wangbo Zhao, Yike Yuan, Jiaqi Wang, Conghui He, Ziwei Liu, et al. Mmbench: Is your multi-modal model an all-around player? In *European conference on computer vision*, pages 216–233. Springer, 2024b.

Liana Mikaelyan, Ayyoob Imani, Mathew Salvaris, Parth Pathak, and Mohsen Fayyaz. Deltallm: Compress llms with low-rank deltas between shared weights. *arXiv preprint arXiv:2501.18596*, 2025.

Piotr Nawrot, Jan Chorowski, Adrian Łaćucki, and Edoardo M Ponti. Efficient transformers with dynamic token pooling. *arXiv preprint arXiv:2211.09761*, 2022.

Bryan A Plummer, Liwei Wang, Chris M Cervantes, Juan C Caicedo, Julia Hockenmaier, and Svetlana Lazebnik. Flickr30k entities: Collecting region-to-phrase correspondences for richer image-to-sentence models. In *Proceedings of the IEEE international conference on computer vision*, pages 2641–2649, 2015.

Alec Radford, Jong Wook Kim, Chris Hallacy, Aditya Ramesh, Gabriel Goh, Sandhini Agarwal, Girish Sastry, Amanda Askell, Pamela Mishkin, Jack Clark, et al. Learning transferable visual models from natural language supervision. In *International conference on machine learning*, pages 8748–8763. PmLR, 2021.

Yongming Rao, Wenliang Zhao, Benlin Liu, Jiwen Lu, Jie Zhou, and Cho-Jui Hsieh. Dynamiccvit: Efficient vision transformers with dynamic token sparsification. *Advances in neural information processing systems*, 34:13937–13949, 2021.

Yuzhang Shang, Mu Cai, Bingxin Xu, Yong Jae Lee, and Yan Yan. Llava-prumerge: Adaptive token reduction for efficient large multimodal models. *arXiv preprint arXiv:2403.15388*, 2024.

Quan Sun, Yuxin Fang, Ledell Wu, Xinlong Wang, and Yue Cao. Eva-clip: Improved training techniques for clip at scale. *arXiv preprint arXiv:2303.15389*, 2023.

Gemma Team, Thomas Mesnard, Cassidy Hardin, Robert Dadashi, Surya Bhupatiraju, Shreya Pathak, Laurent Sifre, Morgane Rivière, Mihir Sanjay Kale, Juliette Love, et al. Gemma: Open models based on gemini research and technology. *arXiv preprint arXiv:2403.08295*, 2024.

Hugo Touvron, Thibaut Lavril, Gautier Izacard, Xavier Martinet, Marie-Anne Lachaux, Timothée Lacroix, Baptiste Rozière, Naman Goyal, Eric Hambro, Faisal Azhar, et al. Llama: Open and efficient foundation language models. *arXiv preprint arXiv:2302.13971*, 2023.

Michael Tschannen, Alexey Gritsenko, Xiao Wang, Muhammad Ferjad Naeem, Ibrahim Alabdulmohsin, Nikhil Parthasarathy, Talfan Evans, Lucas Beyer, Ye Xia, Basil Mustafa, et al. Siglip 2: Multilingual vision-language encoders with improved semantic understanding, localization, and dense features. *arXiv preprint arXiv:2502.14786*, 2025.

Kaichen Zhang, Bo Li, Peiyuan Zhang, Fanyi Pu, Joshua Adrian Cahyono, Kairui Hu, Shuai Liu, Yuanhan Zhang, Jingkang Yang, Chunyuan Li, et al. Lmms-eval: Reality check on the evaluation of large multimodal models. In *Findings of the Association for Computational Linguistics: NAACL 2025*, pages 881–916, 2025.

Qizhe Zhang, Aosong Cheng, Ming Lu, Zhiyong Zhuo, Minqi Wang, Jiajun Cao, Shaobo Guo, Qi She, and Shanghang Zhang. [cls] attention is all you need for training-free visual token pruning: Make vlm inference faster. *arXiv preprint arXiv:2412.01818*, 2024.